PROCEEDINGS B

royalsocietypublishing.org/journal/rspb

Research

Cite this article: Esteve J, Hughes NC. 2023 Developmental and functional controls on enrolment in an ancient, extinct arthropod. *Proc. R. Soc. B* **290**: 20230871. https://doi.org/10.1098/rspb.2023.0871

Received: 13 April 2023
Accepted: 19 May 2023

Subject Category:
Palaeobiology

Subject Areas:
palaeontology, developmental biology, biomechanics

Keywords:
biomechanics, kinematics, ontogeny, tagmosis, trilobites, Silurian

Authors for correspondence:
Jorge Esteve
e-mail: jorgeves@ucm.es
Nigel C. Hughes
e-mail: nigel.hughes@ucr.edu

Electronic supplementary material is available online at https://doi.org/10.6084/m9.figshare.c.6673504.

THE ROYAL SOCIETY PUBLISHING

Developmental and functional controls on enrolment in an ancient, extinct arthropod

Jorge Esteve[1] and Nigel C. Hughes[2]

[1]Departamento de Geodinámica, Estratigrafía y Paleontología, Facultad de CC. Geológicas, Universidad Complutense de Madrid, 28040, Madrid, Spain
[2]Department of Earth and Planetary Sciences, University of California, Riverside, CA 92521, USA

Three-dimensional models reveal how the mechanics of exoskeletal enrolment changed during the development of a model organism for insights into ancient arthropod development, the 429-million-year-old trilobite *Aulacopleura koninckii*. Changes in the number, size and allocation of segments within the trunk, coupled with the need to maintain effective exoskeletal shielding of soft tissue during enrolment, necessitated a transition in enrolment style about the onset of mature growth. During an earlier growth phase, enrolment was sphaeroidal, with the venter of the trunk fitting exactly against that of the head. In later growth, if lateral exoskeletal encapsulation was to be maintained trunk length proportions did not permit such exact fitting, requiring an alternative, non-sphaeoridal enrolment style. Our study favours the adoption of a posture in later growth in which the posterior trunk extended beyond the front of the head. This change in enrolment accommodated a pattern of notable variation in the number of mature trunk segments, well known to characterize the development of this species. It suggests how an animal whose early segmental development was remarkably precisely controlled was able to realize the marked variation in mature segment number that was related, apparently, to life in a physically challenging, reduced oxygen setting.

1. Introduction

As a tool for glimpses into the behaviour of extinct organisms, virtual biomechanical modelling [1–6] is most effective when the parameters of the model are well constrained by biological data [6,7]. In this paper, we apply the exceptionally well-known growth morphometry of the ancient arthropod *Aulacopleura koninckii* [8–13], along with data from rare specimens preserved uncompressed in enrolled posture (figure 1*a–c*), to reveal how the changing shape and construction of the organism during ontogeny apparently resulted in a change in the style in which the animal enrolled when assuming defensive posture.

Thousands of complete exoskeletons of *Aulacopleura koninckii* are preserved within a 1.4 m thick interval of siltstone near Loděnice in the Czech Republic [14]. As these are both well preserved and span much of post-embryonic development, the species serves as an informal but informative 'model animal' for aspects of development in early arthropods, particularly those related to the development of the number, form and sizes of trunk segments (see below) [8–12]. Like most other trilobites, *A. koninckii* is known to have enrolled on occasions [8] (figure 1*d–e*), most probably as a defensive posture. At Loděnice, all enrolled specimens have been flattened during sediment compaction (figure 1*e–l*), but several specimens are known from nearby localities that are preserved uncompacted in limestone. Of these NMP-L12807 presents an exceptionally well-preserved case as the nearly entire dorsal exoskeleton, barring the posteriormost trunk, is preserved enrolled in original relief. This specimen reveals not only sclerite proportions, but also articulation angles between adjacent segments during enrolment. Based on the assumption that this specimen preserves a posture typical of enrolled forms at its developmental stage and that enrolment was laterally encapsulated throughout growth, we apply the

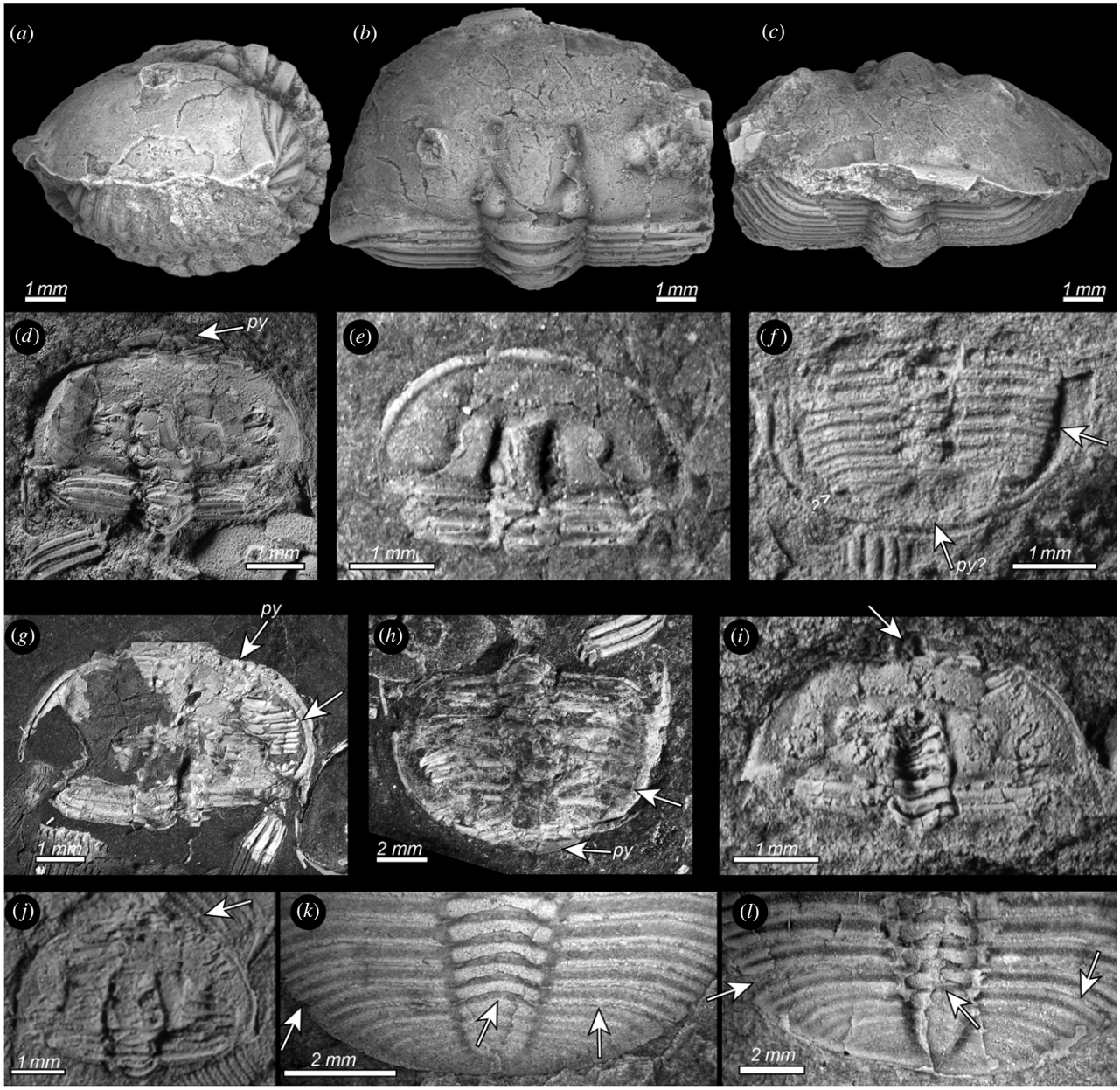

Figure 1. (*a–j*) Enrolled specimens of *Aulacopleura koninckii* from the Silurian of the Czech Republic. (*a–c*) NMP-L12807, lateral (*a*), dorsal (*b*) and frontal views (*c*) of the three-dimensionally preserved holaspid enrolled specimen used to create the three-dimensional models (see text for explanations). (*d–l*) Flattened enrolled specimens. (*d*) CGS-2130 showing the ventral side of the pygidium (py) resting below the cephalon in an external spiral enrolment configuration. (*e*) NMP-P4257389 with flexure of the two anteriormost thoracic segments visible. (*f*) NMP-P4257389 with pleural tips fitting into the ventral doublure furrow (arrow), and missing pygidium (py?). (*g*) CGS-5790 with flexure of rear part of trunk, and thus posteriormost segments and the pygidium hidden beneath the cephalon in typical spiral enrolment configuration, with pleural tips fitting into ventral doublure furrow (arrow). (*h*) CGS-5790 with dorsal side of pygidium (py) resting below cephalon showing an external spiral enrolment configuration, with pleural tips fitting into ventral doublure furrow (arrow). (*i*) CGS-2130 broken glabella reveals ventral side of thoracic segments and posteriormost trunk (arrow), and suggesting sphaeroidal enrolment. (*j*) CGS-JV13401 broken fixigena reveals ventral side of thoracic segments and the posteriormost trunk (arrow), and suggesting sphaeroidal enrolment. (*k,l*) Posterior trunk segments incompletely released from pygidium in *Aulacopleura koninckii* from the Silurian of Czech Republic. (*k*) CGS-P2096 segment apparently released on right side and axial ring (arrows) but remaining fused to the pygidium on left side (arrow). (*l*) NMP-L39401 with segment apparently released on right side and axial ring (arrows) but remaining fused to the pygidium on left side (arrow).

methods of Esteve *et al*. [15,16] to build three-dimensional digital reconstructions of *A. koninckii* that can be digitally manipulated to explore the range of biomechanically possible stances across a wide range of ontogenetic stages. These models shed new light on changes of functional morphology during ontogeny, and into the kinematics required for enrolment at each developmental stage.

A particular advantage of the Loděnice collection of *A. koninckii* is that it spans an unusually wide range of developmental stages (Sn), including multiple successive instars of the immature, *meraspid* period during which the thorax sequentially acquired additional segments at a rate of one per moult stage, and the following *holaspid* period during which the number of segments in the thorax remained constant between subsequent instars, or nearly so (see Fusco [13] and Hughes *et al*. [10] for detailed examination of ontogeny of this animal). An additional curiosity of *A. koninckii* is that the species shows five varieties (morphotypes) of holaspid form, which are distinguished by their number of mature thoracic segments and that range from 18 (t18) to 22 (t22) thoracic segments. These attributes provide the unique opportunity to explore whether enrolment style changed as

the animal developed, and how the variation evident among mature forms might relate to this.

Here we consider and evaluate three styles of enrolment that may have applied in this animal: (i) sphaeroidal enrolment in which the ventral rim of the posterior trunk fits exactly the ventral rim of the cephalon [17,18], (ii) internal spiral enrolment in which the posterior trunk is curled inside the cephalic venter [17,18] and (iii) external spiral enrolment in which the distal margins of the posterior trunk and anterior pygidium are buttressed against the ventral surface of the cephalon and the posterior of the pygidium extends beyond the anterior of the cephalon [19].

2. Constraints on the model

An holaspid specimen (NMP-L12807) preserved enrolled without compaction shows the position and arrangement of pleural tips with respect to the cephalic venter in enrolled posture (figure 1*a–c*). This, coupled with measurement of the axial ring lengths of individual segments and the degree of flexure between adjacent segments in the same specimen, provided a guide for modelling enrolment style both in animals at this particular developmental stage, and across various ontogenetic stages. Such modelling assumed that the pleural tips fitted against the rim of the cephalic doublure during enrolment throughout ontogeny, an assumption consistent with the condition in flattened enrolled meraspid and holaspid specimens (figure 1*e–l*).

Given the assumption of a conserved profile for the great majority of the trunk during enrolment at all stages of development, the average degree of flexure between adjacent tergites would necessarily have been greater in specimens with fewer trunk segments (electronic supplementary material, figures S1 and S2, and movies SM1–SM11). Although the model for enrolment used here depends on the pattern in NMP-L12807 being general, this can be verified, within limits, by examining whether the model would yield any exposed gaps between the rear of a tergite and the anterior of the articulating half-ring of the subsequent tergite at any developmental stage or, alternatively, whether solid sclerite surfaces would interpenetrate one another during enrolment. Given the protective function of the exoskeleton, soft tissue exposure upon enrolment is unlikely to have occurred, and interpenetration would clearly be impossible. The model for enrolment derived from NMP-L12807 did not result in either exposure or interpenetration at any stage and is thus consistent with our assumption.

The trunk of this animal maintained a constant rearward-increasing growth gradient throughout the interval of growth considered in this study, with individual segment size determined by its position with respect to this gradient [11]. This gradient formed the basis of a modelled ontogenetic progression for the growth of the tergites of this animal which informed our geometric model building [10]. An estimate of individual tergite length per stage was derived from detailed morphometric analysis of hundreds of specimens from the meraspid stage with five thoracic segments onwards up to the size of the largest holaspid [11,12].

3. Material and methods

(a) Materials

For the three-dimensional shape reconstruction, a three-dimensionally preserved and articulated specimen (NMP-L12807) from the Liteň Formation at Loděnice was scanned at the National Museum in Prague by X-ray micro-tomography using a SkyScan 1172 at 141 µA and 70 kV with Al + Cu Filter. N-Recon Software (Bruker) was used for reconstruction (electronic supplementary material, Dataset S1 and three-dimensional model of NMP-L12807). A second three-dimensionally preserved specimen, from Kozel, is housed at the Museum of Comparative Zoology, Harvard University (MCZ103482, Schary and Krantz collections) [8] (figure 1*d*); however, this specimen is slightly compressed and consequently is not suitable for the kinematic analysis. All studied specimens are housed at the collections of the National Museum, Cirkusová 1740, Prague 9, Czech Republic (prefix NMP-L/P) and the Czech Geological Survey, Klárov 3, Prague 1, Czech Republic (prefix CGS/JV). A combination of pictures and photogravimetry of three-dimensional prone specimens preserved in limestone including CGS2185 and CGS-JV14949 from Na Černidlech Hill near Loděnice, and CGS-JV1708 from Lištice allowed us to model the missing rear trunk of NMP-L12807 (see electronic supplementary material, three-dimensional models in Blender B1–B11). Flattened enrolled specimens from Na Černidlech Hill include CGS1359, CGS2130, CGS2130, CGS2169, CGS5790, CGL-JV14964, NMP-L39947, NMP-L39979, NMP-L39988, NMP-L39989, NMP-P4257380, NMP-P4257381, NMP-P4257382, NMP-P4257385, NMP-P4257387, NMP-P4257389.

(b) Fossil three-dimensional modelling

The open-source three-dimensional graphics software MeshLab (http://www.meshlab.net/) was used to visualize the mesh and was then imported into the open-source three-dimensional graphics and animation software Blender (https://www.blender.org/). This was done so that different morphological elements could be digitally distinguished and their relative movements inferred, informing the computer models of enrolment. Using Blender, we then retopologied (i.e. retopology is a procedure for simplifying the topology of a mesh to make it cleaner and easier to work with) each sclerite to complete the missing parts and to obtain an accurate but lower resolution three-dimensional model which described the geometry of the original scanned specimen. In the resulting model, we define a 'rig' for each sclerite that allowed us to individually describe its kinematics and to manipulate it independently of other sclerites, according to the constraints described above. Following the known functional morphology related to trilobite enrolment (see [15–17]), we assigned the centre and axis of rotation to the anterior edge of each trunk pleura, which fits below the posterior edge of the previous segment. The variation around the axis of rotation for successive segments was obtained with the following logarithmic expression which, in polar coordinates, can be written as $\mathrm{Ln}[\,a(i)]b$, where a and b are two variables and depend on the particular enrolment style (or stage in our case), i is a counter for successive segments [15] (electronic supplementary material, table S1). The angles between segments yielding enrolment were derived from NMP-L12807, and using these and tergite lengths, we were able to derive a logarithmic expression of the trunk curvature during enrolment that was also compatible with geometry of prone (i.e. naturally outstretched) specimens at the same developmental stage. Using these same parameters, we then reverse modelled, deriving tergite lengths from prone specimens and using the same geometric profile upon enrolment to ensure that, when the model enrolled this specimen, the result matched that of the original enrolled specimen. Segment length data applied in our models were based primarily on the modelled data from an *A. koninckii* with 22 segments in the holaspid phase, as this was the maximum number observed in the species. We then built a series of three-dimensional models for individuals at meraspid instars (= numbers of thoracic segments) 5, 10, 15 respectively, and then for individuals entering the mature growth phase (i.e. holaspid growth identified by the number of instars

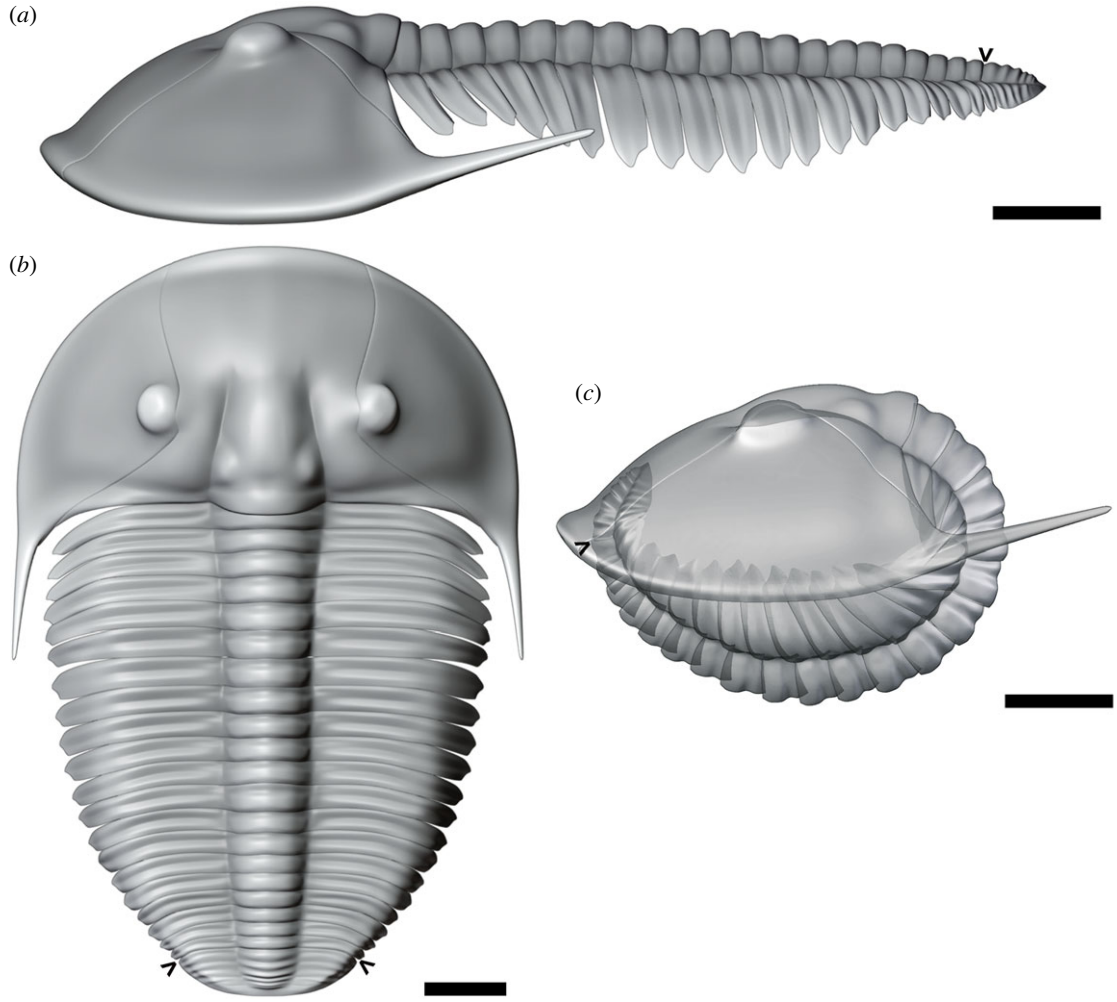

Figure 2. (*a–c*) Three-dimensional S20-t20 model of *Aulacopleura koninckii* from the Silurian of Czech Republic based in NMP-L12807 (see text for explanation). (*a*) Prone model in lateral view. (*b*) Prone model in dorsal view. (*c*) Enrolled model in lateral view. S = instar stage after the first meraspid stage (=S0), t = morphotype according to number of thoracic segments. Arrows point the border between the thorax and the pygidium. Scale bar = 1 mm.

following release of the first thoracic segment) with segment lengths computed from Fusco *et al*. [11], equating to specimens with occipital-glabellar lengths greater than 1.4 mm. Scans and the resulting three-dimensional reconstructions (electronic supplementary material, data S1–S11) are provided in the electronic supplementary material.

4. Results

Three-dimensional models (figure 2–4; electronic supplementary material, figures S1 and S2, and movies M1–M11) built for a series of developmental stages according to the constraints discussed above show that, given modelled segment ontogeny and a conserved, simple logarithmic function guiding flexure throughout the trunk, meraspid enrolment was able to position the border of the trunk exactly under the cephalic border, yielding sphaeroidal enrolment. However, flexure observed beyond the approximately 18th thoracic segment (figure 3*a*) requires a different pattern, with alternatives related to whether the trilobite tucked the rear trunk inside the cephalon (internal spiral enrolment), or whether it extended it beyond the cephalic anterior (external spiral enrolment).

In internal spiral enrolment, each of the posteriormost thoracic segments tucked inside the cephalic vault would show an elevated and equal degree of flexure markedly greater than those segments immediately preceding them. A sharp increase in the flexure of the posterior trunk would be required at the onset of spiral enrolment because the pygidium itself, being made of fused segments, allowed no internal flexure in itself. Given the physical constraints mentioned above, in *A. koninckii* such a transition from sphaeroidal to internal spiral enrolment type would accompany transition into the holaspid S18 t18 stage and would maintain encapsulation.

According to the internal spiral model, the extent to which the posterior trunk penetrated the cephalic vault increased during subsequent growth stages, especially as the trunk segment-rich *A. koninckii* morphotypes continued to add additional trunk segments for several more stages, and as existing segments increased in size during the subsequent moults of all morphotypes. The kinematic plots showing the angle of flexure between adjacent thoracic segments follow a simple log function up to S18 but changed notably thereafter (figure 3*a*,*b*).

In our reconstruction (figure 3; electronic supplementary material, figures S1 and S2), those posteriormost thoracic segments with elevated and equal degrees of flexure in internal spiral enrolment show consistent angles of flexure for those morphs that achieved 19, 20 and 21 thoracic segments as their maximum number. For those that achieved 22 thoracic segments, the angle of curvature was a little higher and those with 18 segments higher still (figure 3*b*). The different patterns for these two 'end-member' morphs are consistent with the

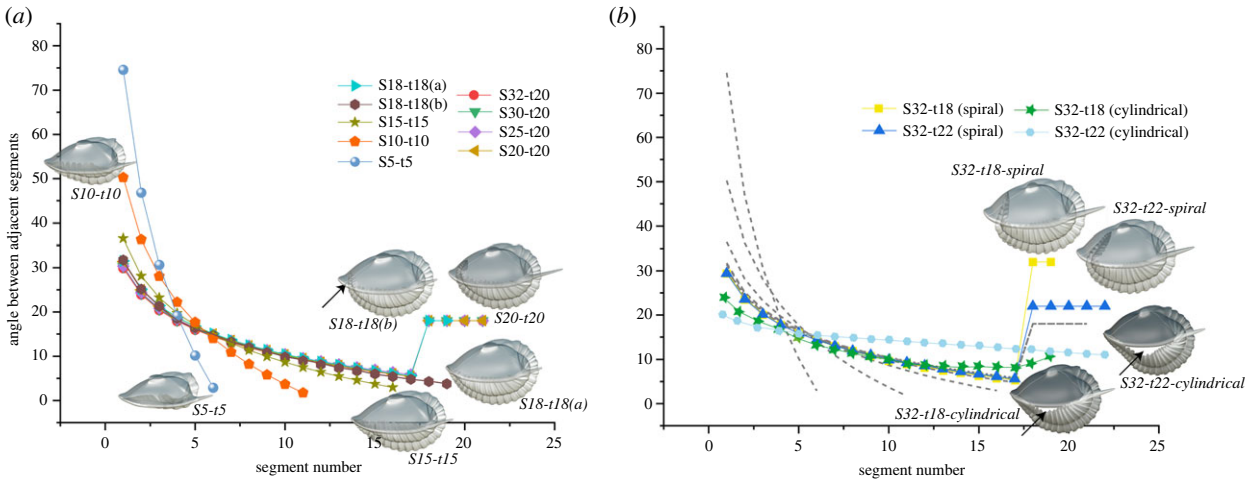

Figure 3. (*a,b*) Kinematic curve showing the articulation angle between successive segments obtained with the expression $\mathrm{Ln}[\,a(i)]b$. (*a*) Models based on individuals with two instars after the onset of the holaspid period. (*b*) Models based on five instars after the onset of the holaspid period. Grey dashed lines in (*b*) correspond with the trajectories of individuals with two instars (electronic supplementary material, table S1).

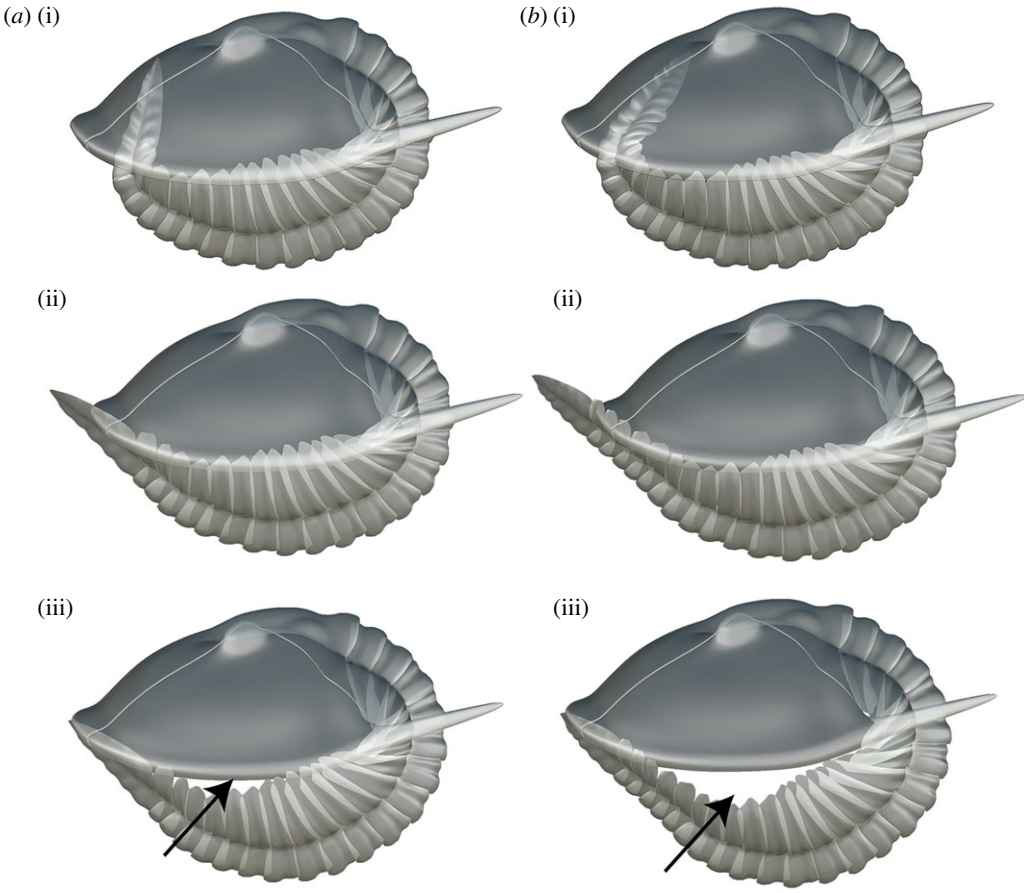

Figure 4. (*a,b*) Three-dimensional models showing possible enrolment postures for latest stage instars of morphotypes with 18 and 22 thoracic segments, respectively, of *Aulacopleura koninckii* from the Silurian of Czech Republic. (*a*) S32-t18, (i) internal spiral enrolment, (ii) external spiral enrolment with pygidium projected beyond the cephalic edge, (iii) cylindrical enrolment with the pygidium resting beneath the cephalon. (*b*) S32-t22, (i) internal spiral enrolment, (ii) external spiral enrolment with pygidium projected beyond the cephalic edge, (iii) cylindrical enrolment with the pygidium resting beneath the cephalon. Arrows point out the gap of non-encapsulated forms (see electronic supplementary material).

following: (i) in the form with 22 segments the greater total number of trunk segments led to a longer total trunk than in other morphs and therefore greater flexure per segment articulation in that region tucked inside the cephalon, and (ii) in the morph with 18 thoracic segments the pygidium transitioned to an alternative growth mode four moults prior to that achieved in forms with 22 segments: a result of it assumed its holaspid pygidial segment growth mode earlier, generating a relatively larger pygidium than in other morphs, the accommodation of which under the cephalic vault required greater flexure in the posteriormost thoracic segments.

Accordingly, logarithmic distribution of flexure regarding all segments operated during sphaeroidal enrolment when the pygidium fit against the cephalic venter, but could not

apply during internal spiral enrolment because of the need to accommodate the inflexible pygidium against the sloped cephalic undersurface.

Internal spiral enrolment is plausible for *A. koninckii* but, in large forms with many segments, requires the posteriormost trunk to extend far inside the cephalic vault (e.g. figure 3*b*, 4*a*i, *b*ii; electronic supplementary material, figure S2). Given that there were internal cephalic organs in this region, including the stomach, this degree of penetration seems surprising. Hence, we considered other possible enrolment strategies.

Requiring the posterior of the trunk match the anterior of the cephalon at all ontogenetic stages for all morphs upon enrolment (figure 4*a*iii, *b*iii) would maintain sphaeroidal enrolment throughout ontogeny. However, when so applied, the exoskeleton failed to fully encapsulate the body upon enrolment in specimens at stage S32-t18 and above, leaving a cylindrical pattern of enrolment with an unprotected gape at the abaxial, lateral margin (figures 3*b*, 4*a*iii, biii). Furthermore, unlike either of the spiral enrolment models (see below), the kinematic curves for this cylindrical enrolment model do not conserve an even gradient in the degree of flexure throughout much of the trunk in the later stages of development (figure 3*b*). This model was thus rejected.

The final alternative considered is that in the more mature forms the posteriormost trunk extended forward of the cephalic anterior upon enrolment, leaving a gape that exposed the pygidial venter (figure 4*a*iii, *b*iii). Such an external spiral enrolment style does not require the posteriormost thoracic segments to flex during such enrolment, i.e. these could show zero degrees of flexure between adjacent segments when obtaining this posture, (figure 4*a*iii, *b*iii). Hence, rather than the sharp increase in the degree of flexure in the posteriormost segment required in the internal spiral mode (figure 4*a*i, *b*i), external spiral posture accords with the consistently declining gradient of flexure from the anterior to the posterior of the trunk based on our observations of NMP-L12807.

5. Discussion

Our kinematic model is based on the profile of enrolment in NMP-L12807 up to the 17 thoracic segment being conserved among all specimens, across all the developmental stages modelled. This assumption is not necessarily valid, as similarly sized members of the same species are known to show some variation in enrolment profile [20] accompanied by minor variation in overall trunk segment number [15,21]. However, in the case of *A. koninckii*, correlations between the changes in enrolment style predicted based on the assumption of a maintained enrolment geometry and other patterns of variation discussed below support this assumption.

Our analysis suggests that in *A. koninckii* a transition in enrolment style took place at the point at which the number and sizes of trunk segments exceeded the possibility for encapsulated sphaeroidal enrolment. As we discount cylindrical enrolment in this form (see above), two alternatives remains: internal spiral enrolment or external spiral enrolment. While internal spiral enrolment would maintain exoskeletal encapsulation, it requires both an abrupt increase in the degree of flexure of the posteriormost thoracic segments, and that the posterior trunk occupied a considerable volume of the cephalic vault. External spiral enrolment, on the other hand, requires no sharp change in the profile of flexure degree between adjacent segments but did not afford complete exoskeletal encapsulation. In order to decide which of these scenarios might have been more likely employed, we consider additional data that is independent of our growth model.

If internal spiral enrolment pertained, it would have placed a premium on efficient, relatively high-angle articulation across segment boundaries in the posterior part of the thorax and at the anterior margin of the pygidium. To permit this greater flexure, the articulating half-rings of these segments are expected to be longer than those immediately anterior to them. They should also have functioned efficiently. Neither of these expectations is met by the data available. Although accurate measurement of individual articulating half-ring lengths across a sufficient sample size is unfeasible due to preservational constraints, no departure from a consistent gradient of declining half-ring length along the trunk is evident to us in any specimen. Nor is there an indication of enlarged longitudinal muscle apodemes in these segments. More tellingly, an unusually large proportion of the total sample of measurable *A. koninckii* specimens reveals trunk segments that commonly remained partially fused along some portion of their length to those posteriors to them (i.e. the articulations between segments are incompletely developed). Such segments could not have permitted flexure at any point along their margins. Given that thoracic segments originate by release from the anterior margin of the meraspid pygidium such cases of fusion are often classed as 'incomplete release' (figure 1*k–l*; electronic supplementary material, figure 3SD). As such segments cannot have permitted flexure, the animals that bore them are highly unlikely to have exhibited spiral enrolment. All known cases of such fusion (which can include up to two conjoined, partly released segments) occur in the posterior thorax of specimens with 18 or more thoracic segments, and none are known either in younger specimens or more anteriorly in the trunk. Although detecting partial release may be challenging in smaller specimens, the fact that fused segments occur only in the posterior portions of specimens with above the minimum number of holaspid segments suggests that such fusion was only preserved in larger specimens. As such fusion occurred in approximately 10% of specimens of this size [14], it appears to have been tolerated among living individuals. Accordingly, while the number and sizes of trunk segments was precisely controlled throughout the development of *A. koninckii*, control of late-stage functional articulation formation was apparently more lax.

As external spiral enrolment would not have required flexure of the posteriormost trunk segments, it is consistent with these observations. The underside of the pygidium extending immediately anterior of the cephalon would have been exposed, and several flattened, enrolled specimens from Na Černidlech Hill show such a condition (e.g. figure 1*d–h*). Although in such cases, the exact position of the posterior trunk was modified taphonomically during sediment compression it seems unlikely that flattening alone could have transformed an internal spirally enrolled specimen into an external spirally enrolled one. A further benefit of the external spiral enrolment type is that due to the contact between the inner part of cephalic doublure and the lateral margins of the posterior thoracic segments and anterior pygidium, lateral shearing would be impeded [19].

Attainment of 18 thoracic segments marked the earliest onset of an important ontogenetic transition in *A. koninckii*: the initiation of the holaspid period of growth, which is defined

by having stable numbers of thoracic segments despite continued moulting [22]. *Aulacopleura koninckii* is remarkable for having five different holaspid morphotypes, which span the range from 18 and 22 thoracic segments. For all morphotypes, including that with 20 thoracic segments in maturity, the transition from sphaeroidal enrolment style invoked herein apparently occurred at or close to the stage with 18 thoracic segments, irrespective of the morphotype. In the case of individuals attaining a maximum of 20 thoracic segments, this would have been two instars before onset of their holaspid stage (figure 3*a*). That transition in enrolment style coincided with the initiation of a major developmental transition in segment expression and trunk tagmosis within the species, is intriguing, as the remarkably variable mature thoracic segment number seen in *A. koninckii* [10] became manifest after the transition from sphaeroidal enrolment had taken place. Both the internal and external spiral enrolment styles offered more latitude in the size and placement of the posteriormost trunk because the constraint of a precise shape match between the cephalon and trunk required for sphaeroidal enrolment became partly relaxed.

Our proposed transition from sphaeroidal enrolment coincides with another notable ontogenetic transition in this species. The majority of specimens of *A. koninckii* from Loděnice are at least partially disarticulated [14, pp. 229–230]. Among such there is a notable change from separated cranidia and free cheeks in specimens up to the size expected to have about 18 thoracic segments, to a mature condition in which the cephalic dorsal suture, although still clearly incised, apparently failed to open during moulting. Thereafter the dorsal elements of the cephalon remained articulated, and moulting was apparently facilitated by opening of the 'neck joint' (see [14], fig. 14A). For reasons unknown, but probably involving movements associated with moulting, onset of failure of the cephalic sutures broadly coincided both with the transition in enrolment mode and with the increasing prevalence of partly fused sutures in the posterior part of the trunk.

These observations suggest that several behavioural traits related to segment articulation changed at a point in ontogeny broadly coincident with the switch in enrolment style. Although overall shape and sclerite proportions were regulated with a notable degree of precision in *A. koninckii* [11,19], onset of the transition to the holaspid/epimorphic stage in this trilobite coincided with several significant changes in life habits. One explanation may be that above a certain size threshold predatory pressure on *A. koninckii* declined, mitigating the need for encapsulated enrolment and succeeded by evident variation in trunk segment numbers and body proportions among mature *A. koninckii* morphotypes. It has been suggested previously that this variability may have been related to the physical challenge of oxygen availability in this environment and gill respiratory capacity [23,24]. More trunk segments presumably implied greater overall gill surface area and, due to the area/volume relationship, the slight gape under the pygidium during external spiral enrolment might have offered more benefit for respiration for large specimens than cost in terms of increased vulnerability.

The variation in enrolment mechanics discussed herein is compatible with the interpretation of *A. koninckii* as an opportunistic trilobite, living at the margins of oxygen availability, where it sporadically 'bloomed' in both overall abundance and that relative to other organisms [14]. It appears that following release from a morphological constraint required by sphaeroidal enrolment *A. koninckii* expressed several developmental pathways, possibly in response to subtle changes in oxygen availability.

Data accessibility. Scanners and the resulting three-dimensional reconstructions (Blender files) are available on Dryad Digital Repository [25].

The data are provided in the electronic supplementary material [26].

Authors' contributions. J.E.: conceptualization, funding acquisition, software, writing—original draft and writing—review and editing; N.C.H.: conceptualization, funding acquisition, supervision, writing—original draft and writing—review and editing.

All authors gave final approval for publication and agreed to be held accountable for the work performed therein.

Conflict of interest declaration. We declare we have no competing interests.

Funding. This paper is a contribution to project PID2021-125585NB-I00 of the Spanish Ministry of Science and Innovation, and to IGCP668 and NSF EAR-1849963.

Acknowledgements. We thank Giuseppe Fusco (University of Padova, Italy), for kindly providing segment length data for *A. koninckii* according to modelled growth, for continued discussion and for his thoughtful comments on an early version of this work. Paul Hong (Korea Institute of Geoscience and Mineral Resources) kindly provided pictures of specimens with incomplete segment release. We are grateful to James Holmes (Uppsala University) and one anonymous reviewer for the revision of this paper, and to Pedro Rubio (Teruel, Spain) for his comments and assistance with the kinematic models. We thank Zuzana Heřmanová (National Museum, Prague) for her assistance with X-ray micro-tomography, and Zuzana Heřmanová and Petr Budil (Czech Geological Survey) for kind access to collections in their care. This paper is dedicated to Jiří Kříž in gratitude for making the series of studies of this animal possible for us.

References

1. Rayfield EJ. 2007 Finite element analysis and understanding the biomechanics and evolution of living and fossil organisms. *Annu. Rev. Earth Planet. Sci.* **35**, 541–576. (doi:10.1146/annurev.earth.35.031306.140104)
2. Gutarra S, Moon BC, Rahman IA, Palmer C, Lautenschlager S, Brimacombe AJ, Benton MJ. 2019 Effects of body plan evolution on the hydrodynamic drag and energy requirements of swimming in ichthyosaurs. *Proc. R. Soc. B* **286**, 20182786. (doi:10.1098/rspb.2018.2786)
3. Song H, Song H, Rahman IA, Chu D. 2021 Computational fluid dynamics confirms drag reduction associated with trilobite queuing behaviour. *Palaeontology* **64**, 597–608. (doi:10.1111/pala.12562)
4. Schmidt M, Melzer RR, Plotnick RE, Bicknell RDC. 2022 Spines and baskets in apex predatory sea scorpions uncover unique feeding strategies using 3D-kinematics. *iScience* **25**, 103662. (doi:10.1016/j.isci.2021.103662)
5. Esteve J, López M, Ramírez CG, Gómez I. 2021 Fluid dynamic simulation suggests hopping locomotion in the Ordovician trilobite *Placoparia*. *J. Theor. Biol.* **531**, 110916. (doi:10.1016/j.jtbi.2021.110916)
6. Schmidt M, Hazerli D, Richter S. 2020 Kinematics and morphology: a comparison of 3D-patterns in the fifth pereiopod of swimming and non-swimming crab species (Malacostraca, Decapoda, Brachyura). *J. Morphol.* **281**, 1547–1566. (doi:10.1002/jmor.21268)
7. Cunningham JA, Rahman IA, Lautenschlager S, Rayfield EJ, Donoghue PCJ. 2014 A virtual world of paleontology. *Trends Ecol. Evol.* **29**, 347–357. (doi:10.1016/j.tree.2014.04.004)
8. Hughes NC, Chapman RE. 1995 Growth and variation in the Silurian proetide trilobite *Aulacopleura konincki* and its implications for

trilobite palaeobiology. *Lethaia* **12**, 333–353. (doi:10.1111/j.1502-3931.1995.tb01824.x)

9. Hughes NC, Minelli A, Fusco G. 2006 The ontogeny of trilobite segmentation: a comparative approach. *Paleobiology* **32**, 602–627. (doi:10.1666/06017.1)
10. Hughes NC, Hong PS, Hou JB, Fusco G. 2017 The development of the Silurian trilobite *Aulacopleura koninckii* reconstructed by applying inferred growth and segmentation dynamics: a case study in paleo-evo-devo. *Front. Ecol. Evol.* **5**, e1–e12. (doi:10.3389/fevo.2017.00037)
11. Fusco G, Hong PS, Hughes NC. 2014 Positional specification in the segmental growth pattern of an early arthropod. *Proc. R. Soc. B* **281**, 20133037. (doi:10.1098/rspb.2013.3037)
12. Hong PS, Hughes NC, Sheets HD. 2014 Size, shape, and systematics of the Silurian trilobite *Aulacopleura koninckii. J. Paleontol.* **86**, 1120–1138. (doi:10.1666/13-142)
13. Fusco G, Hughes NC, Webster M, Minelli A. 2004 Exploring developmental modes in a fossil arthropod: Growth and trunk segmentation of the trilobite *Aulacopleura koninckii*. *Am. Nat.* **163**, 167–183. (doi:10.1086/381042)
14. Hughes NC, Kříž J, Macquaker JHS, Huff WD. 2014 The depositional environment and taphonomy of the Homerian '*Aulacopleura* shales' fossil assemblage near Loděnice, Czech Republic (Prague Basin, Perunican microcontinent). *Bull. Geosci.* **89**, 219–238. (doi:10.3140/bull.geosci.1414)
15. Esteve J, Rubio P, Zamora S, Rahman IA. 2017 Modelling enrolment in Cambrian trilobites. *Palaeontology* **60**, 423–432. (doi:10.1111/pala.12294)
16. Esteve J, Gutiérrez-Marco JC, Rubio P, Rábano I. 2018 Evolution of trilobite enrolment during the Great Ordovician Biodiversification Event: insights from kinematic modelling. *Lethaia* **51**, 207–217. (doi:10.1111/let.12242)
17. Esteve J. 2013 Revisión del enrollamiento en los trilobites del Cámbrico español y su implicación en la evolución de los trilobites. *Estud. Geol.* **69**, 209–225. (doi:10.3989/egeol.41215.259)
18. Suárez MG, Esteve J. 2021 Morphological diversity and disparity in trilobite cephala and the evolution of trilobite enrolment throughout the Palaeozoic. *Lethaia* **54**, 752–761. (doi:10.1111/let.12437)
19. Lerosey-Aubril R, Angiolini L. 2009 Permian trilobites from Antalya Province, Turkey, and enrollment in late Palaeozoic trilobites. *Turkish J. Earth Sci.* **18**, 427–448. (doi:10.3906/yer-0801-5)
20. Fortey RA, Owens RM. 1975 Proetida: a new order of trilobites. *Foss. Strat.* **4**, 227–239.
21. Esteve J, Zamora S, Gozalo R, Linán E. 2010 Sphaeroidal enrolment in middle Cambrian solenopleuropsine trilobites. *Lethaia* **43**, 478–493. (doi:10.1111/j.1502-3931.2009.00205.x)
22. Raw F. 1925 The development of *Leptoplastus sateri* (Calloway) and of other trilobites (Olenidae, Ptychopariidae, Conocoryphidae, Paradoxidae, Phacopidae, and Mesonacidae). *J. Geol. Soc.* **81**, 223–324. (doi:10.1144/GSL.JGS.1925.081.01-04.12)
23. Hou JB, Hughes NC, Hopkins MJ. 2021 The trilobite upper limb branch is a well-developed gill. *Sci. Adv.* **7**, eabe7377. (doi:10.1126/sciadv.abe7377)
24. Jackson ISC, Budd GE. 2017 Intraspecific morphological variation of *Agnostus pisiformis*, a Cambrian Series 3 trilobite-like arthropod. *Lethaia* **50**, 467–485. (doi:10.1111/let.12201)
25. Esteve J, Hughes NC. 2023 Data from: Developmental and functional controls on enrolment in an ancient, extinct arthropod. Dryad Digital Respository. (doi:10.5061/dryad.wh70rxwsk)
26. Esteve J, Hughes NC. 2023 Developmental and functional controls on enrolment in an ancient, extinct arthropod. Figshare. (doi:10.6084/m9.figshare.c.6673504)